Coherent radar detection in log-normal clutter

A. Farina, A. Russo and F.A. Studer

Abstract: The paper deals with the problem of radar detection of a target echo embedded in log-normal clutter and white Gaussian noise. Relevant features of this article, with respect to previous papers on the same subject, refer to the coherent model assumed for the clutter and the processing chain. In more detail, the in-phase and quadrature components of clutter have been modelled to give a log-normal amplitude distribution and a near uniform distribution of the phase. Any shape of the correlation among consecutive clutter samples is also allowed in the model. At the same time, the processing chain is also coherent, i.e. it operates on the two components of the signals. Two architectures have been considered for the processor. The first, used in current practice, is formed of a linear transversal filter (for the clutter attenuation and the target echo enhancement) cascaded with a quadratic envelope detector and a comparison with a suitable threshold. The second processor considered differs from the previous one in the filter for clutter cancellation. A nonlinear homomorphic filter has been conceived to obtain a better suppression of clutter. The detection performance of the two processing chains have been evaluated, by means of computer simulation, in a number of operational cases of interest. The paper gives a first contribution to the problem of finding better models of disturbance and of deriving more efficient processing chains.

1 Introduction and review of previous research

The detection of targets in clutter is one of the most relevant problems in the radar technique. An abundance of papers and books have been published on this topic; Schleher [1] gives a commented collection of the most important publications. The theory of optimum detection of targets embedded in clutter is well established when the probability density of clutter amplitude is Rayleigh or, in other words, the in-phase and quadrature components are jointly Gaussian-distributed processes, for any shape of the clutter autocorrelation function. The optimum processor for the suppression of clutter and enhancement of target echo is a coherent linear filter, cascaded with a modulus extractor and a comparison with a suitable threshold. A detailed description of the optimum processor and the evaluation of performance are described in References 2 and 3 (pp. 139–141), and a summary of relevant equations can be found in the 'outline of MTI theory' of Reference 1 (pp. 20–35).

In several practical applications, clutter amplitude is not Rayleigh-distributed. These situations occur when sea clutter is viewed with a high-resolution radar (pulse width $\tau < 0.5 \ \mu s$) at low grazing angle ($\phi < 5$ degrees). They also result when land clutter is viewed at low grazing angles ($\phi < 5$ degrees), regardless of radar resolution. In these cases, the probability density function exhibits a long tail ('spiky' clutter); in other words, there is a significant probability of having very large returns from a clutter patch. The mechanism of spikyness is well understood now from a physical point of view [4, 5, 29]. Three non-Rayleigh probability density functions for the clutter amplitude have been proposed: log-normal, Weibull [1, 5] and K-distribution [6, 7].

Agreement on which model performs best has not yet been reached. A comparison of the results predicted from the theory with the experiments does not seem to be resolvable, owing to the large number of parameters (frequency, pulse length, beamwidth, polarisation, siting and environmental conditions) involved. A number of

papers refer experimental results on non-Rayleigh clutter; see, for example, the commented collection of papers in Reference 8 (section 5) or Reference 9. More recently, Perry [10] refers to measurements made by a 3-D radar on ground and valley clutter showing a Weibull amplitude distribution. References 11–19 refer to detailed sea clutter measurement experiments. They confirm the spiky nature of sea clutter; in addition, they provide an analysis of the correlation properties in the space and time domains. Spiky sea clutter, as evidenced by amplitude distributions having long tails, is most evident for horizontal polarisation, low grazing angles, high spatial resolution of the radar and for the up- and downwind directions. The amplitude distribution is also often observed to be independent of sea state as such.

The optimum processor for non-Rayleigh clutter is no longer a linear filter, and it has not yet been found. The detection performance of conventional processors in non-Rayleigh clutter generally deteriorates from that in Rayleigh clutter [8]. This is due to the long 'tail' of the distribution, which results in a problematic setting of the detection threshold. In fact, an increase of false alarm rate should be expected or, alternatively, a reduction of detection probability should occur in order to maintain CFAR characteristics.

The list of References at the end of this paper suggests a considerable amount of work has been done in the area of processing non-Rayleigh clutter. Some of the important published studies are critically examined in this Section.

Consider first the problem of processing log-normal clutter. In References 20 and 21, the clutter has been modelled as a noncoherent (i.e. only the amplitude was considered) process, uncorrelated from pulse to pulse; thermal noise has been neglected. Operating only on the clutter amplitude, the processor has been considered noncoherent. A number of conventional receivers (namely linear, logarithmic, binary integrator and median detector) have been compared in terms of detection performance. In addition, the performance of the optimum processor, under the above-mentioned hypotheses, has been found by evaluating the Chernoff bound. Among the processors considered, the logarithmic receiver has been recommended, owing to the good detection performance achieved, the high dynamic range provided to handle the wide range of clutter amplitude and its CFAR capability in Rayleigh-distributed clutter.

In Reference 22, the detection performance of a coherent MTI cascaded with a quadratic detector has been evaluated when fed with a correlated coherent log-normal clutter. Such a clutter has been generated by correlating separately the log-normal amplitude and then tagging it with uniform, independent phase values. With this questionable clutter model, the performance of a single MTI has been derived, neglecting the thermal noise, and a measure of the performance degradation with respect to the Rayleigh clutter has been found. However, as Schleher points out, the comparison of MTI performance with respect to log-normal and Rayleigh clutter is unfair because the spectra of the two clutter models are different, since the effect of the nonlinearity on the spectrum of the log-normal clutter is not accounted for. As a matter of fact, the log-normal correlated clutter model suggested by Schleher does not allow the separate shaping of the probability density and autocorrelation functions.

Reference 23 affords the problem of detecting targets, having log-normal amplitude, embedded in log-normal clutter. This problem arises in harbour surveillance radars. These radars are characterised by large antenna apertures and short transmitted pulse width, necessary to provide the high definition required for precise navigation in narrow channels. In addition, the radar is usually situated so that both sea clutter and vessels are viewed at relatively low grazing angles. The above-stated conditions give rise to a log-normal probability density of the amplitudes for both target and clutter. The noncoherent processor examined in this case is the cascade of an envelope detector, a logarithmic device and a moving window. The detection performance has been evaluated considering independent clutter samples and neglecting thermal noise.

An explicit account of thermal noise in addition to log-normal clutter is only given by Fante [25], in which, however, simplifications concerning the clutter fluctuations are made. Specifically, two cases are considered, namely: the completely correlated or completely uncorrelated clutter samples on a pulse-to-pulse basis.

As far as the prediction of detection performance in Weibull clutter is concerned, Schleher [26] provides a comparison between the linear receiver, the logarithmic receiver, the binary integrator and the median detector. Optimum performances are estimated by means of the Chernoff bound. Furthermore, in the Weibull case, the modelling is confined to the amplitude of clutter. Additionally, independence between clutter samples is assumed and thermal noise is neglected.

Similar remarks concerning the noncoherent processing of clutter can be derived for the clutter distributed according to the K-law [16, 18].

This paper affords the problem of target detection in log-normal clutter. For this special case, all the previous limitations are overcome. In more detail, a coherent model is assumed for the clutter and the processing chain. As far as the clutter model is concerned, the in-phase and quadrature components of clutter have been modelled to give a log-normal amplitude distribution and a near-uniform distribution of the phase. Any shape of correlation among consecutive clutter samples is allowed in the model. It is worthwhile noting that the probability density and the autocorrelation functions can be separately shaped at will.

Additionally, thermal noise is taken into proper consideration. At the same time, the processing chain is also coherent, i.e. it operates on the two components of the signals. Two architectures have been considered for the processor. The first, used in current practice, is formed of a linear transversal filter (for clutter attenuation and target

echo enhancement) cascaded with a quadratic envelope detector and a comparison with a suitable threshold. The filter can be an MTI device and a coherent integrator or the optimum filter [27] for the case of clutter having Gaussian probability density. The second processor considered differs from the previous one in the filter for clutter cancellation. A nonlinear homomorphic filter has been conceived to obtain a better suppression of clutter. The detection performance of the two processing chains have been evaluated, by means of computer simulation, in a number of operational cases of interest. It will be noted that the processor currently used in practice suffers poor detection performance; better results are achievable with the second processor considered.

The paper gives a first contribution to the problems of finding better models of disturbance and of deriving more efficient processing chains. The remainder of the paper is organised as follows. Section 2 illustrates the mathematical model assumed for the clutter, the relevant properties of the model and the method of generating correlated log-normal clutter in the computer simulation. Section 3 describes the detection performance obtained with the current-practice processing chain. In Section 4, the nonlinear processing chain is derived and the detection performance evaluated and compared with the other cases. In the closing Section 5, the limitations of the present analysis are pointed out and the trends of future research are envisaged. In particular, the theory for deriving the optimum detection for any kind of target model embedded in any kind of clutter model is briefly illustrated, postponing the description of the theory in Reference 28. The paper is corroborated with an extensive list of References covering the last 20 years.

2 Coherent model for log-normal clutter

The purpose of this Section is to detail the mathematical model assumed to represent the coherent samples of log-normal clutter. Consequently, the algorithm adopted to generate clutter samples for the computer simulation is also derived. In particular, it is shown how correlated samples of log-normal clutter can be obtained by suitably processing coherent samples of white Gaussian noise.

The Section is organised as follows. In subsection 2.1 the well known results relevant to the modelling of the log-normal amplitude of a single clutter echo are briefly summarised. In subsection 2.2 an original extension regarding the modelling of the in-phase and quadrature components of a single clutter echo is provided. Particular attention is devoted to the selection of the probability density of the echo phase. In more detail, comparison is made, in terms of detection performance, between the effect of having either a Gaussian or a uniform distribution of the clutter phase.

In subsection 2.3 a further extension of the mathematical model of the clutter, pertaining to the coherent pulse train case, is presented. The model is conceived around the structural separability of nonlinearity from memory. In other words, the model is the cascade of a generator of white Gaussian noise, a linear dynamic filter and a nonlinear memoryless device.

Rather than resorting to physical considerations it is preferred to justify the model by showing that it is a canonic approach for representing a stochastic coherent process having any shape of probability density and autocorrelation functions. Other two additional considerations are related to the corresponding simplicity in simulating

69

the clutter process and, more important, the capability of deriving the processor which has an architecture replying in some respect that of the model. The latter property is well known and widely used in the field of Gaussian-distributed clutter processes. In this case, the model of the clutter consists of a linear filter fed by a white Gaussian noise; the main part of the corresponding processor results to be a linear filter with parameters strictly dependent on the parameters of the clutter model (whitening filter).

In subsection 2.4, the previous theory is applied to the simulation of correlated coherent log-normal clutter samples. Indications of the number of statistical trials to be carried out are also given.

2.1 Noncoherent single pulse case

It is well known [20] that a real-valued, log-normal-distributed, random variable r can be obtained from a Gaussian-distributed variable n, having mean value $\bar{n}$ and standard deviation σ, by applying the transformation

$$r = \exp(n) \tag{1}$$

Consequently, the probability density function (PDF) of r turns out to be

$$p(r) = \frac{1}{\sqrt{(2\pi)}\sigma r} \exp\left\{-\frac{\ln^2(r/m)}{2\sigma^2}\right\} \tag{2}$$

where m represents the median value of r, related to $\bar{n}$ as $m = \exp(\bar{n})$, and σ is referred to as the 'logarithmic standard deviation' of r. The moments of r depend on m and σ as

$$E\{r^k\} = m^k \exp\left\{\frac{k^2\sigma^2}{2}\right\} \tag{3}$$

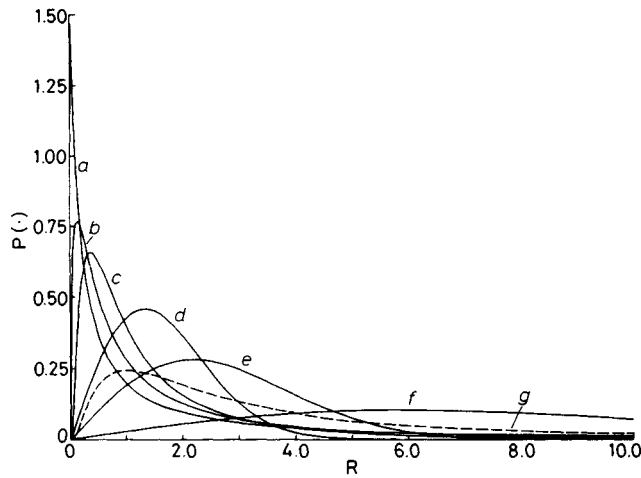Examples of log-normal probability density functions are represented in Fig. 1, for $m = 1$ and different values of σ. It

Fig. 1 *Probability density functions for Rayleigh and log-normal amplitudes*

a Log-normal $(m = 1, \sigma = 2, \bar{r} = e^2)$ *e* Rayleigh $(\bar{r} = e)$
b Log-normal $(m = 1, \sigma = \sqrt{2}, \bar{r} = e)$ *f* Rayleigh $(\bar{r} = e^2)$
c Log-normal $(m = 1, \sigma = 1, \bar{r} = \sqrt{e})$ *g* Log-normal $(m = e, \sigma = 1, \bar{r} = e^{3/2})$
d Rayleigh $(\bar{r} = \sqrt{e})$

is evident that an increase in σ results in a longer tail for the PDF, together with a higher and narrower peak, closer to the null value. For comparison purposes, the corresponding Rayleigh PDFs having the same mean values are also depicted in the same Figure. The long tail that characterises the log-normal PDF accounts for the phenomenon of spiky clutter, with large amplitude values having a significant probability of occurrence. The probability of crossing a threshold value T for a log-normal-distributed

random variable is

$$P_{LN}(T) = \frac{1}{2} - \text{erf}\left\{\frac{\ln(T/m)}{\sigma}\right\} \tag{4}$$

where $\text{erf}(\cdot)$ denotes the error function:

$$\text{erf}(x) = \frac{1}{\sqrt{2\pi}} \int_0^x \exp\left\{-\frac{t^2}{2}\right\} dt \tag{5}$$

For comparison, the probability $P(T)$ for a Rayleigh-distributed random variable is [8]

$$P_{Ray}(T) = \exp\left\{-\frac{T^2}{2\sigma^2}\right\} \tag{6}$$

Eqns. 4 and 6 are plotted against T in Fig. 2 for a same mean value of the two distributions, namely setting

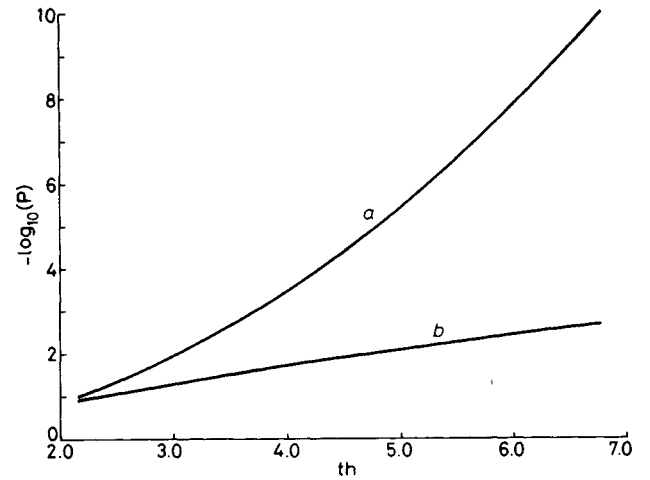$$\sigma_{Ray} = \sqrt{\frac{2}{\pi}} \exp\left\{-\frac{\sigma_{LN}^2}{2}\right\}$$

Fig. 2 *Probability of threshold crossing for Rayleigh and log-normal amplitudes*

a Rayleigh $(\sigma = \sigma_{Ray})$ *b* Log-normal $(m = 1, \sigma = \sigma_{LN})$

A dramatic increase in $P(T)$ is shown, when the log-normal amplitude is considered, with respect to the Rayleigh distribution.

Since the log-normal power depends on two parameters (m, σ), both are relevant for the power associated to a clutter sample, as shown by eqn. 3 for $k = 2$. It is questionable whether m or σ or both should be used to account for clutter power in a log-normal model. The effect of taking a value $m = e$ (with $\sigma = 1$) is also shown in Fig. 1; this results in the same power as $m = 1$, $\sigma = \sqrt{2}$, but a rather different PDF (broken line). When considering a coherent model, the two assumptions lead to rather different results; the former (i.e. taking $m = 1$ and increasing σ with clutter power) has been chosen in this paper, as will be clarified in Section 2.2. This choice may be somewhat different from others in the technical literature where the clutter power is related essentially to the median value.

2.2 Coherent single pulse case

The problem of modelling log-normal coherent clutter is now afforded in two steps. At first, the case of single pulse (i.e. random variable generation) is considered; then (Section 2.3) the theory is extended to the pulse train case (i.e. stochastic process). In order to model coherent clutter samples having a log-normal-distributed amplitude, the PDFs of the in-phase and quadrature components must be specified. This is achieved by resorting to an extension of the transformation (eqn. 1) to the complex field. Let x, y be

two jointly Gaussian-distributed, zero-mean random variables, and define the complex-valued random variable

$$z = x + jy \qquad (7)$$

A complex-valued log-normal random variable can be defined as

$$w = u + jv = \text{cexp}\,(z) = (\exp\,(x))(\cos\,y + j\,\sin\,y) \qquad (8)$$

where cexp $(\cdot)$ stands for the complex exponential function. The amplitude of w depends on x only:

$$|w| = \exp\,(x)$$

and is log-normal-distributed, according to eqns. 1 and 2; the phase of w coincides with the Gaussian y:

$$\arg\,(w) = y \qquad (9)$$

It is common to model noise or clutter samples as having a uniformly distributed phase in $(0, 2\pi)$, corresponding to the absence of any *a priori* information about the phase values and a circular symmetry in the PDF of the complex variate. The Gaussian PDF assumed in this paper for arg (w) does not rely on a physical model, but is motivated by the dramatic simplifications in the development of the mathematical model; this is particularly true for the pulse train case, which is considered in Section 2.3. It is worth specifying that arg (w) is considered to be defined on the whole real axis, where the Gaussian PDF applies. However, since the phase is always considered through trigonometric functions, a sort of 'aliasing effect' arises for its PDF, in that the probabilities of values of arg (w) congruent modulo 2π add up. Consequently, a nearly uniform distribution of arg (w) (mod 2π) results, at least when σ_y is large. This reconciles the mathematical model with the common assumption.

The statistics of w are easily computed [30] as (see Appendix)

$$E\{w\} = \left\{\exp\left(\frac{\sigma_x^2 - \sigma_y^2}{2}\right)\right\}(\cos\,\sigma_{xy} + j\,\sin\,\sigma_{xy}) \qquad (10)$$

$$E\{|w|^2\} = \exp\,\{2\sigma_x^2\} \qquad (11)$$

where σ_x^2, σ_y^2 and σ_{xy} denote the second-order moments of the Gaussian variates x and y. The joint PDF of the in-phase and quadrature components u, v of w has been computed by carefully applying the transformation theorem [31] (see Appendix). In particular, assuming that x and y are independent $(\sigma_{xy} = 0)$ and having equal power $(\sigma_x^2 = \sigma_y^2 = \sigma^2)$, the joint probability of (u, v) is

$$p(u, v) = \frac{1}{2\pi|w|^2\sigma^2}\exp\left\{\frac{\ln^2\,|w|}{2\sigma^2}\right\}$$
$$\cdot \sum_{k=-\infty}^{+\infty}\exp\left\{-\frac{(\arg_0\,(w) + 2k\pi)^2}{2\sigma^2}\right\} \qquad (12)$$

where $\arg_0\,(w)$ is defined in $[-\pi, +\pi]$ as the principal value of the argument; namely

$$\arg_0\,(w) \triangleq \tan^{-1}\,(v/u) + \frac{\pi}{2}\,\text{sign}\,(v)(1 - \text{sign}\,(u)) \qquad (13)$$

and sign $(\cdot) = \pm 1$, according to the sign of the argument. From eqn. 12 it is apparent that u, v are not independent of each other; however, they are mutually uncorrelated [32]; the marginal distributions of u and v have been computed via numerical integration [32]. Examples of $p(u)$ and $p(v)$ are drawn in Figs. 3 and 4, respectively. It turns out that $p(v)$ is an even function, whereas u has unit mean

value (eqn. 10) and a nonsymmetric PDF. The variances of u and v are both equal to $\frac{1}{2}(\exp\,(2\sigma^2) - 1)$.
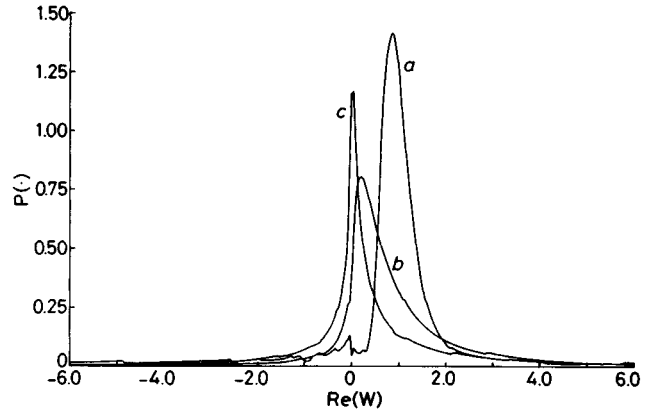
Fig. 3 *Probability density function of in-phase component*
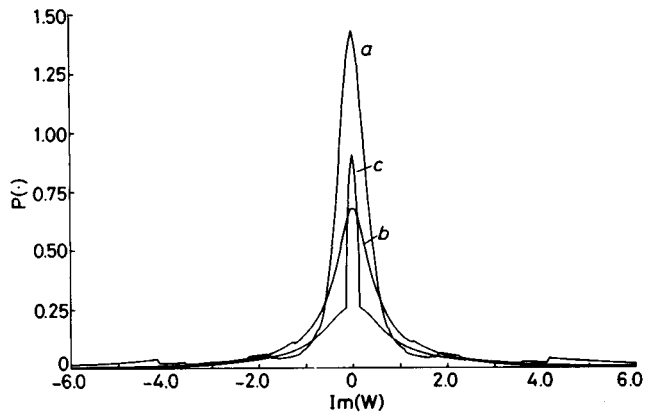$a\ \sigma^2 = 0.1 \qquad b\ \sigma^2 = 1 \qquad c\ \sigma^2 = 3$

Fig. 4 *Probability density function of quadrature component*
$a\ \sigma^2 = 0.1 \qquad b\ \sigma^2 = 1 \qquad c\ \sigma^2 = 3$

It is possible to conceive a more general model, by allowing x and y to have nonzero mean values $\bar{x}$, $\bar{y}$. This results [32] in a coherent sample having mean value

$$E\{w\} = \{\exp\,(\bar{x})\}(\cos\,\bar{y} + j\,\sin\,\bar{y})$$

and variance

$$\sigma_w^2 = \{\exp\,(2\bar{x})\}(\exp\,(2\sigma^2) - 1)$$

while the median value of the echo amplitude becomes

$$m = \exp\,\{\bar{x}\}$$

This allows representing clutter power as arising from two contributions, one deterministic and the other random. The power ratio between the two terms is given by

$$\frac{\sigma_w^2}{|E\{w\}|^2} = \exp\,(2\sigma^2) - 1$$

However, a deterministic term is not of great concern, since it can be easily filtered out by means of a conventional canceller. Hence, for the sake of simplicity, it is assumed that $\bar{x} = \bar{y} = 0$ throughout the paper. The coherent model discussed in the present Section, and the homomorphic filter presented in Section 4, can easily be extended to the more general case.

Consider now in some detail the case in which the random phase of the clutter, i.e. arg (w), has a uniform distribution in $[-\pi, +\pi]$. The purpose is to compare in a simple way this situation with that considered up to now, i.e. Gaussian distribution of the clutter phase. One possibility would be to evaluate the PDF of $p(u)$ and $p(v)$ and

compare them with those of Figs. 3 and 4. Another method, preferred here, is to show that the detection performance (obtained by processing only one received sample) does not appreciably depend on the distribution of the clutter phase.

To this end, consider the problem of detecting a target embedded in log-normal clutter and white Gaussian noise, by processing only one sample. The target signal is assumed to be known *a priori* except the initial phase; SNR is the value of the signal/noise ratio. The clutter amplitude is log-normal-distributed (with $m = 1$ and σ evaluated from eqn. 3) and with phase either Gaussian or uniform distributed. CNR is the value of the clutter/noise ratio; the same CNR values have been assumed in the two cases, i.e. relevant to the different distribution of the clutter phase. The sum of the in-phase and quadrature components of the noise, clutter and target signal (in the H_1 hypothesis) have been simulated in a digital computer by means of the Monte Carlo technique. In the same program, the processor (i.e. modulus extraction and comparison with a suitable threshold T) has been simulated.

The detection performance, i.e. P_D against SNR for a certain value of CNR and P_{FA}, has been obtained. It is found that these detection curves are stepwise: in other words, below a certain SNR* value the probability of detection is nearly zero, while for SNR values immediately greater than SNR* the corresponding P_D is about 99%. The interesting result obtained is that the detection curves are independent of the distribution of clutter phase (i.e. Gaussian or uniform), and the SNR* values are the same. Table 1 gives the SNR* values against CNR (ranging from

Table 1: Minimum SNR values giving $P_D = 0.99$

CNR, dB	SNR*, dB	T
10	35	51
20	49	256.2
30	60	930.8

Random phase of clutter is either Gaussian or uniform. P_{FA} is assumed to be 10^{-4}; the corresponding threshold value T is shown

10 dB to 30 dB) for $P_{FA} = 10^{-4}$. The corresponding values of the threshold T have also been indicated. Another simulation exercise has been carried out by considering a target having a Rayleigh amplitude and a uniform random phase. The target is embedded in log-normal clutter (having either uniform or Gaussian phase) and white Gaussian noise. The detection performance corresponding to the processing of a single pulse has been evaluated (see Table 2). Two main results are obtained, namely (i) the detection

Table 2: P_D values against SNR values for a target having a Rayleigh amplitude and uniform phase

CNR = 10 dB		CNR = 20 dB		CNR = 30 dB	
SNR, dB	P_D, %	SNR, dB	P_D, %	SNR, dB	P_D, %
30	7.4	45	10.8	55	6.2
35	44.2	50	49.8	60	42.3
40	76.7	55	79.6	65	75.5
45	91.9	60	93.1	70	91.5
$T = 51$		$T = 265.2$		$T = 930.8$	

Clutter amplitude is log-normal and phase is either Gaussian or uniform

curves are not stepwise but smoothed and (ii) the detection curves differ, at the maximum, by 0.1% when considering either Gaussian or uniform distribution of the clutter phase. The results obtained confirm that the hypothesis of Gaussian distribution of the clutter phase is equivalent to

uniform phase assumption. A Gaussian phase is preferred in this paper, owing to the possibility of generating a correlated coherent log-normal pulse train, as is shown in Section 2.3.

2.3 Correlated coherent pulse train case

The concept of correlating noncoherent log-normal samples has been discussed [33, 34]. The basis of the approach is to feed with a white Gaussian noise a proper linear dynamic filter cascaded with an exponential nonlinearity. It is worthwhile noting that sometimes the methods for deriving the parameters of the filter, starting from the probability density and autocorrelation functions required, are tortuous.

The concept of a coherent log-normal continuous-time process with specified autocorrelation function is now introduced with the purpose of modelling the coherent pulse train case (i.e. discrete-time sequence). Assume that $x(t)$ and $y(t)$ are zero-mean, real-valued, jointly Gaussian-distributed stationary processes, and denote with $R_{xx}(t)$, $R_{yy}(t)$ and $R_{xy}(t)$ their auto- and crosscorrelation functions. These processes can be thought of as the in-phase and quadrature components of a complex-valued Gaussian process $z(t)$, with autocorrelation function

$$R_{zz}(t) = R_{xx}(t) + R_{yy}(t) - j(R_{xy}(t) - R_{yx}(t)) \qquad (14)$$

A straightforward extension of eqn. 8 provides the definition of the complex-valued, log-normal process:

$$w(t) = \text{cexp } (z(t)) \qquad (15)$$

having a mean value (eqn. 10) given by

$$E\{w(t)\} = \left\{ \exp\left(\frac{R_{xx}(0) - R_{yy}(0)}{2}\right) \right\}(\cos R_{xy}(0) + j \sin R_{xy}(0)) \qquad (16)$$

and autocorrelation function [30] given by

$$R_{ww}(t) = \text{cexp } (R_{xx}(t) + R_{yy}(t) + R_{xx}(0) - R_{yy}(0)$$
$$-j(R_{xy}(t) - R_{yx}(t))) \qquad (17)$$

Eqns. 14–17 provide the fundamental relationships for the development of the coherent log-normal clutter model in the continuous-time case. The clutter process $w(t)$ is represented as the output of a nonlinear memoryless transformaton (eqn. 15) operating on a Gaussian process $z(t)$. The latter process $z(t)$, in turn, is obtained as the output of a linear filter which shapes $R_{zz}(t)$ having white Gaussian noise at the input [27]. It should be remarked that the ability of obtaining a log-normal-correlated clutter sequence is strongly related to the availability of the 'complex exponential function' which operates on a 'coherent Gaussian process'. Conversely, whether the nonlinear memoryless device is different or its feeding sequence is non-Gaussian, the upstream dynamic filter would be nonlinear, thus invalidating the whole canonical method.

A schematic diagram of the proposed model is depicted in Fig. 5. This model is claimed here to provide a 'canonical' [35, 36] representation of a non-Gaussian process; hence its application can be extended to represent other processes, provided that a suitable nonlinear memoryless function can be found, to replace the cexp ($\cdot$). For each specific application, the nonlinear device is such that it transforms a pair of jointly distributed Gaussian variates into a complex vector having a specified PDF for the amplitude and a Gaussian (but near-uniform) phase. It is explicitly noted that the shape of the clutter autocorrelation function $R_{ww}(t)$ is determined by the combined effect

of the linear filter and nonlinear transformation, as expressed by eqn. 17. In addition, the proposed method
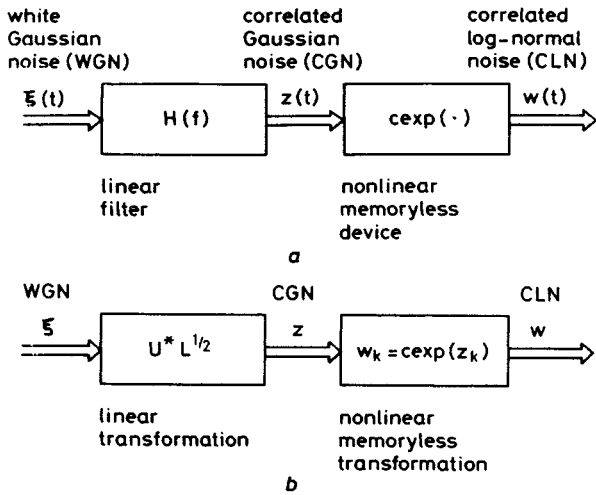

Fig. 5 *Proposed model for correlated log-normal noise*
a Continuous-time model   *b* Discrete-time model

allows control of the shape of the probability density independently of the shape of the autocorrelation function.

A major problem concerning the proposed clutter model is that from a specified autocorrelation function $R_{ww}(t)$ it is necessary to find the corresponding function $R_{zz}(t)$ for the Gaussian input, as well as the parameters $R_{xx}(0)$ and $R_{yy}(0)$. In other words, it is necessary to solve the inverse of eqn. 17, implying evaluation of a logarithm in the complex field, i.e. a multiple-values function. Thus, the existence and uniqueness of the solution cannot be generally guaranteed for an arbitrary $R_{ww}(t)$. A similar problem, i.e. of unrealisable autocorrelation function, was pointed out in Reference 35, where a pair of theorems were derived to deal with this topic; however, they are not easily extensible to the complex field (i.e. the coherent case).

A futher problem refers to the synthesis of the shaping filter for the required autocorrelation function $R_{zz}(t)$. In general, this could be achieved by resorting to standard synthesis techniques for FIR or IIR filters. This will be afforded in the case of discrete-time processes, for which it is possible to resort to eigenvalue/eigenvector decomposition of the process covariance matrix. The proposed approach yields a model that can be easily implemented in a computer, for Monte Carlo simulation purposes.

In order to give some insight in the proposed model, consider in some more detail eqns. 14–17. Assume first that $R_{xy}(t)$ is identically zero and that $x(t)$ and $y(t)$ have the same power. As a result, the deterministic component of $w(t)$ (eqn. 16) is real and equals unity. It contributes to the frequency spectrum of $w(t)$ as a Dirac pulse at zero frequency, with unitary amplitude. The random components of $w(t)$, say $\tilde{w}(t)$, has a real-valued autocorrelation function (see eqn. 17):

$$R_{\tilde{w}\tilde{w}}(t) \triangleq \text{cov } \{w(t)\} = \exp (R_{xx}(t) + R_{yy}(t)) - 1 \qquad (18)$$

corresponding to a symmetric frequency spectrum around zero, and has a power

$$R_{\tilde{w}\tilde{w}}(0) = \exp (R_{xx}(0) + R_{yy}(0)) - 1 = \sigma_w^2 \qquad (19)$$

It can also be shown [31] that, under the above-mentioned hypotheses, $w(t)$ is a wide-sense stationary baseband random process.

A white log-normal process is obtained when $z(t)$ is white Gaussian noise, namely bypassing the shaping filter in the model of Fig. 5.

Letting $R_{xy}(t)$ be nonzero and nonsymmetric yields a complex-valued, time-invariant deterministic component, and a complex-valued autocorrelation function for the random component, which may account for an offset in the frequency spectrum with respect to zero (e.g. due to a nonzero mean-value Doppler frequency). Finally, letting $R_{xx}(0)$ and $R_{yy}(0)$ be different from each other (i.e. allowing unbalanced power between the in-phase and quadrature components at the input) changes the deterministic component of $w(t)$, according to eqn. 16, and affects the random component for an amplitude factor.

For completeness, it is necessary to mention a slightly different approach to account for an offset in the frequency spectrum of the clutter. Assume that x and y are mutually independent, so that $w(t)$ has a real-valued autocorrelation function, and hence a frequency spectrum symmetric around zero. If $w(t)$ is further multiplied by a deterministic phasor cexp $(j2\pi f_c t)$, the resulting signal has a mean Doppler frequency f_c, while still retaining the same PDF and shape of the spectrum. With this approach, the schematic diagram of Fig. 5a should be completed by inserting a complex multiplier downstream the nonlinear device. The applicability of such model may be broader than that of the original model. However, it will not be considered in this paper, since a zero-mean Doppler frequency is assumed for the clutter.

The extension of the proposed model to discrete-time processes is now outlined, which allows modelling of a train of N echoes obtained in response to consecutive radar pulses. A succession of Gaussian-distributed complex-valued variates $z_k = x_k = x_k + jy_k$, is considered, in lieu of the continuous-time process $z(t) = x(t) + jy(t)$. The complex-valued, log-normal-distributed samples are obtained by applying the transformation (eqn. 8) to each Gaussian variate. It is convenient to introduce vector notation to represent the time sequences, namely

$$z = (z_1 z_2, \ldots, z_N)^T$$
$$w = (w_1 w_2, \ldots, w_N)^T \qquad (20)$$

The correlation between consecutive samples is represented by means of the covariance matrices

$$M_z = E\{z^* z^T\}$$
$$M_w = E\{\tilde{w}^* \tilde{w}^T\} \qquad (21)$$

where $\tilde{w}$ denotes the random component of w, namely

$$\tilde{w} = w - E\{w\} \qquad (22)$$

Assuming that the in-phase and quadrature components of z have the same power, the relationship between the corresponding elements (m, n) of M_z and M_w results from eqns. 14, 17 and 21, and is given by

$$[M_w]_{m, n} = \text{cexp } [M_z]_{m, n} - 1 \qquad (23)$$

Consequently, from a specified covariance matrix M_w, it is possible to determine the required covariance matrix M_z for the Gaussian variates. A batch of N samples having the desired covariance matrix M_z can be obtained from a batch of white Gaussian noise samples by means of a suitable linear operator, provided that M_z is Hermitian. In this case, it is possible to perform a decomposition of M_z as follows [27]:

$$M_z = ULU^{T^*} \qquad (24)$$

where L is the diagonal matrix formed with the eigenvalues of M_z and U is the matrix of the corresponding

eigenvectors. Consequently, the linear operator

$$A = U^* L^{1/2} \qquad (25)$$

provides the required transformation from a vector of unitary power white noise to the desired process z (see Fig. 5b).

It can easily be verified that any Hermitian matrix M_z produces a Hermitian matrix M_w, and vice versa, as follows from eqn. 23. However, the matrix M_z does not always turn out to be positive-definite, and hence suitable to represent the covariance matrix of a discrete-time process. As an example, consider the case of a wide-sense stationary log-normal clutter having power P for its random component and a Gaussian-shaped autocorrelation function; assume that a nonzero mean Doppler frequency f_c exists, and let ρ cexp $(j\phi)$ denote the correlation between any two consecutive pulses:

$$\rho \text{ cexp } (j\phi) = \rho(\cos \phi + j \sin \phi) = \frac{E\{\tilde{w}_n^* \tilde{w}_{n+1}\}}{P} \qquad (26)$$

The following covariance matrix M_w is obtained for two pulses:

$$M_w = P\begin{pmatrix} 1 & \rho e^{j\phi} \\ \rho e^{-j\phi} & 1 \end{pmatrix} \qquad (27)$$

The corresponding covariance matrix M_z turns out to be

$$M_z = \begin{bmatrix} \ln(1+P) & \ln|1 + P\rho e^{j\phi}| + j \arg_0 (1 + P\rho e^{j\phi}) \\ \hline \ln|1 + P\rho e^{j\phi}| - j \arg_0 (1 + P\rho e^{j\phi}) & \ln(1+P) \end{bmatrix} \qquad (28)$$

In the case of a clutter spectrum centred at zero Doppler frequency ($\phi = 0$), the matrix M_z is Hermitian, with positive eigenvalues

$$\lambda_1 = \ln(1+P) + \ln(1+P\rho)$$

$$\lambda_2 = \ln(1+P) - \ln(1+P\rho) \qquad (29)$$

since $P > 0$ and $\rho < 1$.

In the more general case (i.e. $\phi \neq 0$), under the condition $P \gg 1$, the eigenvalues of M_z are

$$\lambda_{1,2} = \ln(P) \pm (\ln^2(P\rho) + \phi^2)^{1/2} \qquad (30)$$

the second term being positive if

$$\phi < (-(\ln \rho)(2 \ln P + \ln \rho))^{1/2} \qquad (31)$$

Hence eqn. 31 defines the admissible clutter parameters for the proposed model in the case of two pulses. As an example, let $P = 100$ and $\rho = 0.99$; eqn. 31 yields $\phi < (0.3)$, corresponding to a mean Doppler frequency of (0.048) PRF. Similarly, it is possible to verify that, for a batch of three pulses, a Gaussian-shaped autocorrelation function and a zero-mean Doppler value, the matrix M_z is positive-definite provided that the following inequality holds:

$$\ln^2(1 + P\rho^4) \ln(1 + P) > 2 \ln^2(1 + P\rho) - \ln^2(1 + P) \qquad (32)$$

This defines the range of P and ρ in which the model applies. As an example, eqn. 32 holds for $P \gtrsim 2$ when $\rho = 0.99$.

Some mathematical expedients [32] can be found in order to extend the range of values in which a solution for M_z exists. They correspond to adding a small white-noise or deterministic component, with power ε, to the log-normal clutter. In terms of the covariance matrix M_w, the former corresponds to adding a constant term ε on the diagonal elements; the latter implies replacing '1' by '1 + ε' in eqn. 23.

2.4 Simulation of coherent log-normal clutter

It is worth concluding this Section with some remarks on the simulation of coherent log-normal clutter in a digital computer, according to the proposed model. The model described in Section 2.3 can be directly applied to generate samples of the clutter process in a simulation program. It is well known that the simulation consists of a number of statistically independent trials, in which samples of the input process are generated by the computer and then processed according to the desired algorithm. From the collected outputs, the probability of occurrence of a significant event, or some statistical parameters of the output distribution, can be estimated. The larger the number of trials, the more accurate is the estimate. The computer is able to generate numbers which appear as drawn from a specified PDF (e.g. Gaussian). The subsequent steps follow closely the scheme of Fig. 5b, namely a linear combination is made of the random numbers generated to produce a batch of correlated inputs; then a nonlinear transformation is performed to obtain log-normal-distributed samples representing the input for the processor under examination. Since only a limited number of input data are generated, the space of the events is not fully covered by the trials. Hence, the tails of the PDF can be poorly reproduced, as they correspond to the less likely events. This is not generally a significant problem when dealing with Gaussian variates. However, for the log-normal clutter model, the 'weight' of such tails is greatly emphasised, as can be inferred from the 'cexp' operation. This makes the faithful reproduction of the Gaussian distribution a key problem, thus requiring a large number of trials to be performed, as well as an accurate check of the statistical behaviour of the random number generators.

To give a flavour of the above-mentioned problem, consider the effect of the selection of the number of independent statistical trials on the evaluation of the improvement factor for a linear MTI with given (e.g. binomial) weights. To this end, consider two clutter sequences having the same power spectral density but different probability density functions, namely Rayleigh and log-normal. Owing to the same spectral densities, the corresponding improvement factor values are equal (the same does not apply to the detection and false alarm probabilities). However, the different probability densities of the two clutter sources call for different numbers of statistical trials to reach the same improvement factor estimated values. This situation is clearly illustrated in Fig. 6; it dramatically emerges that the log-normal clutter requires a considerable number of independent trials, i.e. several hundreds of thousands, which will be the normal situation for all the operational cases illustrated in the following Sections.

3 Performance evaluation of conventional processor

The optimum receiver, according to the Neyman-Pearson criterion, maximises the detection probability for a given

74

value of probability of false alarm. Its design requires evaluation of the likelihood ratio, for the observed signal,
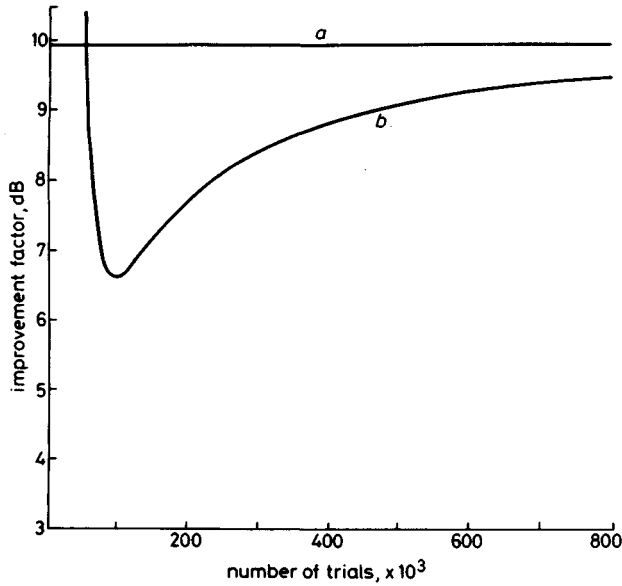

Fig. 6 *Estimated improvement factor (IF) values against number of independent statistical trials*

Clutter/noise power ratio CNR = 20 dB, one-step correlation coefficient $\rho = 0.9$, number of processed pulses $N = 2$; binomial MTI; Swerling 2 model assumed for target
a Rayleigh clutter   *b* Log-normal clutter

comparing the alternative hypotheses of target absent (H_0) or present (H_1). For an input disturbance having Gaussian PDF, it is well known that the optimal receiver consists of a linear filter, followed by an amplitude detector and a threshold [2]. The linear filter provides cancellation of the correlated disturbance (clutter) as well as matched filtering (for *a priori* known target), thus maximising the signal/noise ratio at the output. The coefficients *w* of the linear filter are uniquely determined from the covariance matrix *M* of the disturbance and the expected target samples *S*, according to the well known equations [2]:

(a) $W = M^{-1}S^*$

(b) $W = U_{min}$ (33)

where U_{min} is the eigenvector of *M* associated to its minimum eigenvalue; weights (a) apply for a deterministic target (completely known except for the initial phase), while weights (b) apply for a Swerling 2 target. In practice, owing to lack of information about the clutter statistics, suboptimal filters are used in lieu of the weights of eqn. 33, resorting to the well known MTD (a) and MTI (b) techniques.

When the input disturbance is not Gaussian-distributed, evaluation of the likehood ratio is not easy, even in the case of a single pulse. Furthermore, the resulting optimal

processor is always nonlinear [8]. The theory of stochastic processes [20] provides the basis for the derivation of the optimal processor. However, the structure of the optimal processor in most cases is not known, and among these still remains the log-normal clutter. Approximate, suboptimal processors can be derived in some cases by resorting to intuition; an example is described and evaluated in Section 4.

The purpose of this Section is to assess the performance of a conventional processor, designed under the assumption of a Gaussian-distributed disturbance, in the presence of log-normal clutter having covariance matrix *M* which is evaluated according to a Gaussian-shaped spectrum. The mismatching between the design model and the actual disturbance statistics is shown to cause severe performance degradation in terms of P_D and P_{FA}. It is worth pointing out that, regardless of the PDF of the input disturbance, the filter that maximises the output signal/noise ratio is uniquely determined by the clutter covariance matrix *M*. However, maximising the signal/noise ratio does not guarantee optimum detection performance when the disturbance is not Gaussian-distributed. In other words, the design of the optimum detector requires knowledge of the whole joint PDF of the input samples, rather than the first- and second-order moments (*S* and *M*) that are sufficient statistics for the Gaussian processes.

A schematic diagram of the conventional processor examined here is represented in Fig. 7. A batch of input samples *z* consisting of log-normal clutter *c*, Gaussian noise *n* and (eventually) target echoes *s*, is fed into the linear filter with weights *w* to produce a scalar output *y* that is envelope-detected and compared with the threshold *T*. In order to assess the detection performance, determination of the PDF of the amplitude of *y* under the hypotheses H_0 and H_1 is required. However, analytical results are not available as closed-form solutions, and the computation of P_{FA} and P_D requires the performing of numerical integration of very complex expressions, even in the case of a single pulse. Thus, performance evaluation has been carried out by means of a simulation on a digital computer. This allows evaluation of P_{FA} and P_D, as well as of the PDF of the output of the envelope detector, in any case of interest. In particular, it has been found that, when the target is absent, the output is approximately log-normal-distributed when few samples are processed in the filter. The output power is reduced, with respect to the input, of an amount corresponding to the improvement factor (IF) provided by the filter. The IF, of course, does not depend on the PDF of the input, but only on its covariance matrix. Hence, it is the same that could be achieved on a Rayleigh-distributed disturbance with the same spectrum. The threshold setting, however, is strongly dependent on the PDF, as illustrated in Fig. 8, where P_{FA} is plotted against the threshold value for a clutter with
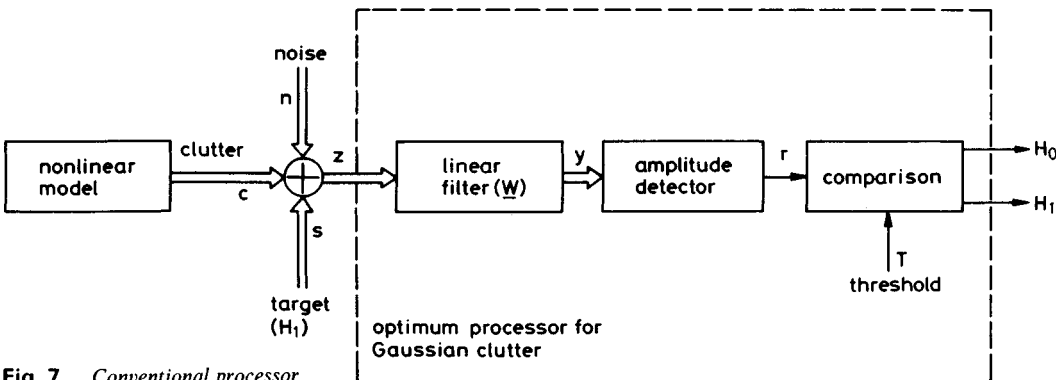

Fig. 7 *Conventional processor*

75

CNR = 30 dB, $\rho = 0.9$; three pulses are processed in the optimal filter with weights (eqn. 33b), providing an IF of
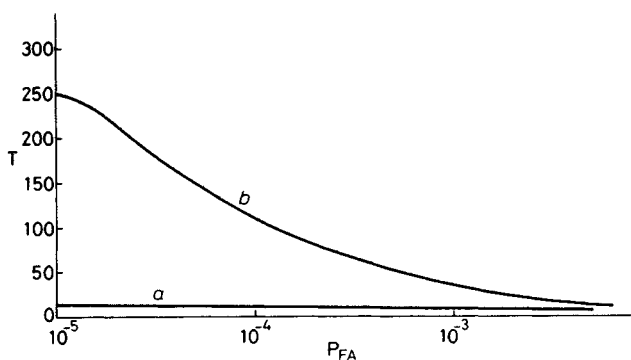

Fig. 8 *Comparison of P_{FA} values against threshold in Rayleigh and log-normal clutter cases*

CNR = 30 dB, $\rho = 0.9$, $N = 3$
a Rayleigh   b Log-normal

18 dB. The Rayleigh case shows an unappreciable variation of T causing dramatic differences in P_{FA}. The log-normal clutter, on the other hand, requires much larger values of T to achieve the same P_{FA}, the difference being emphasised when P_{FA} decreases. The variation of the threshold values with the number of processed pulses and the clutter correlation coefficient is found to follow the corresponding variation of IF.

When the target signal is present, the PDF of the envelope of y assumes the shape illustrated in Fig. 9, which
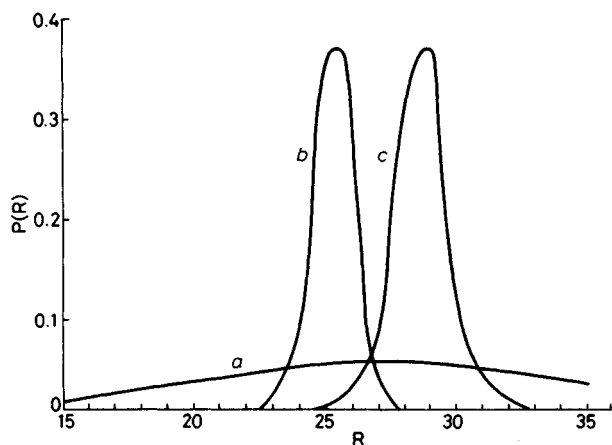
Fig. 9 *Log-normal clutter amplitude after linear coherent filtering*

Rayleigh amplitude shown for comparison; CNR = 30 dB, $\rho = 0.9$, $N = 2$
a Rayleigh clutter, SNR = 25 dB
b Log-normal clutter, SNR = 25 dB
c Log-normal clutter, SNR = 26 dB

pertains to the processing of two pulses, with CNR = 30 dB, $\rho = 0.9$ and a target echo with SNR = 25 dB. The optimum filter with weights (eqn. 33b) provides 10 dB of IF. The PDF in the presence of log-normal clutter differs significantly from that relating to Rayleigh clutter, shown in Fig. 9 for comparison, the latter being much broader. In Fig. 9, the PDF for log-normal clutter and SNR = 26 dB is also represented. It is noteworthy that a difference of 1 dB causes a remarkable shift of the PDF. Consequently, it is expected that for the same threshold value (e.g. $T = 26$), a significant change of P_D is produced from few percent to near unity, when the SNR increases from 25 to 26 dB.

Consider now, in Figs. 10–15, the detection probability P_D represented against the single pulse SNR at the input. The target is assumed to have a constant amplitude and unknown initial phase (Swerling 0) and a Doppler frequency $f_D = 0.5$ PRF. The filter is the optimal one (eqn.

33a). The clutter is assumed to have at the input, on a single pulse, CNR = 30 dB and $\rho = 0.9$. Different values of P_{FA} and of the number of processed pulses are considered.
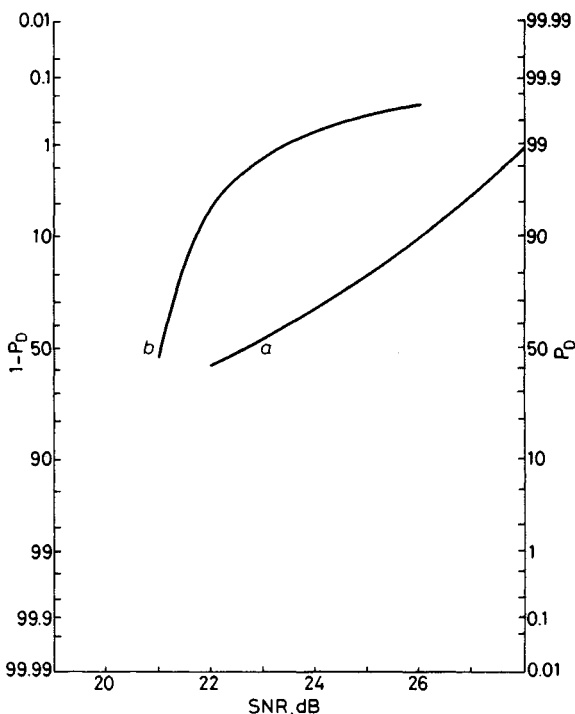

Fig. 10 *Comparison of detection performance of a Swerling 0 target embedded in log-normal and Rayleigh clutter*

CNR = 30 dB, $\rho = 0.9$, $N = 2$, $P_{FA} = 1.5 \times 10^{-2}$
a Rayleigh clutter   b Log-normal clutter

Fig. 10 refers to a high value of P_{FA} (i.e. 1.5×10^{-2}) and $N = 2$ pulses. In this case, the processor performs better against log-normal clutter than against Rayleigh clutter, for a wide range of values of P_D (greater than 50%). This apparently strange phenomenon can be explained by resorting to Fig. 9; to obtain a P_{FA} value of 1.5×10^{-2}, the threshold value should be 16. However, when the required P_{FA} is lowered, as shown in Fig. 11 ($T = 38$), the
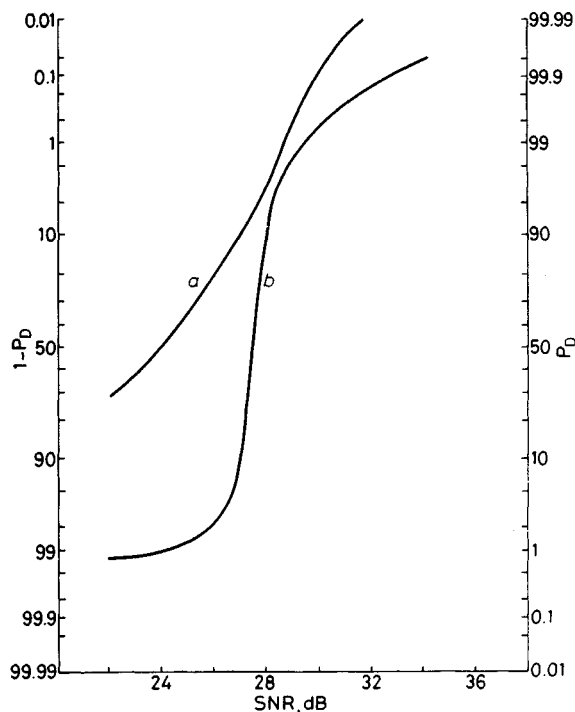

Fig. 11 *As Fig. 10, but with lower P_{FA} value of 5×10^{-3}*
a Rayleigh   b Log-normal

situation reverses; for extremely low P_{FA}, as shown in Fig. 12, the difference of sensitivity in favour of the Rayleigh
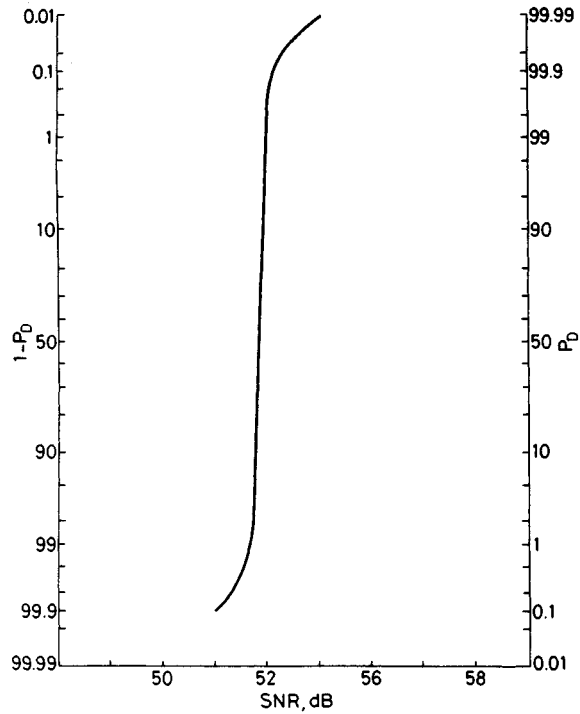

Fig. 12 *As Fig. 10, but with lower P_{FA} value of 2.8×10^{-5}*

Only the 'log-normal' curve is shown, requiring tens of decibels more than the 'Rayleigh' curve

clutter is of the order of tens of decibels. This situation (with P_{FA} ranging between 10^{-4} and 10^{-6}) is typically of interest in radar systems.

A further remark concerns the shape of the curve of P_D against SNR for the log-normal clutter that is nearly stepwise, this feature being enhanced as P_{FA} decreases. In particular, Fig. 12 shows that at the output of the linear filter (providing an IF of 13 dB), a signal/disturbance ratio of about 39 dB (corresponding to SNR = 52 dB at the input)
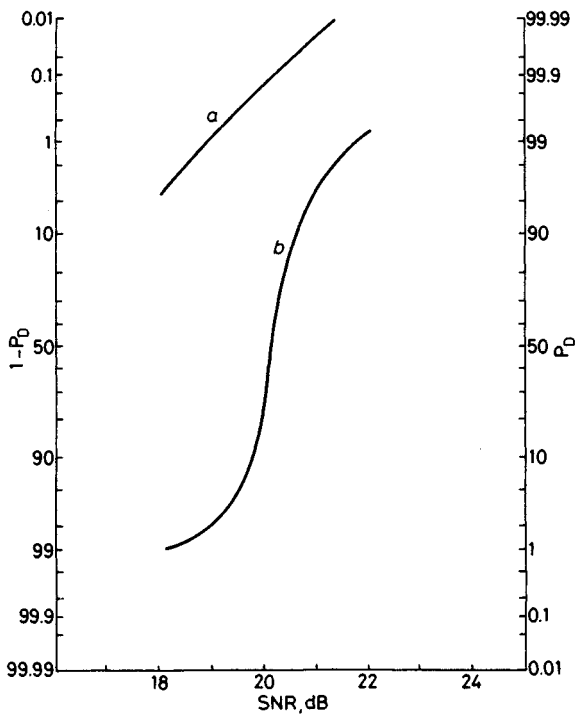
is required to achieve a high P_D (greater than 99%). However, a reduction of 1 dB is enough to drop P_D to less than 1%.

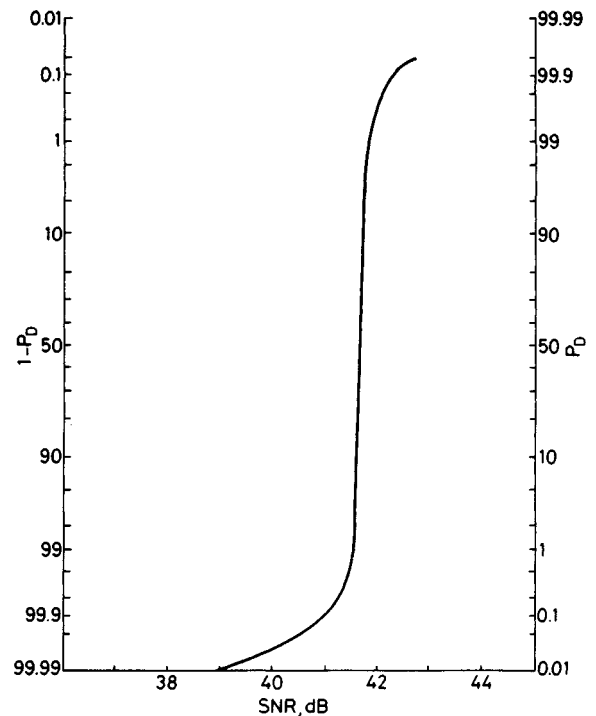Figs. 13, 14 and 15 allow evalution of the effect of

Fig. 14 *Detection performance of a Swerling 0 target model in log-normal clutter for processing of three pulses*

'Rayleigh' curve not shown, requiring tens of decibels less; CNR = 30 dB, $\rho = 0.9$, $N = 3$, $P_{FA} = 2.8 \times 10^{-5}$

increasing the number of pulses. In particular, Fig. 13 refers to three pulses and can be compared with Fig. 11. It is shown that a saving of SNR required to achieve a given P_D is 9–10 dB for the Rayleigh clutter as against 6–8 dB for the log-normal clutter. Similarly, Figs. 12, 14 and 15
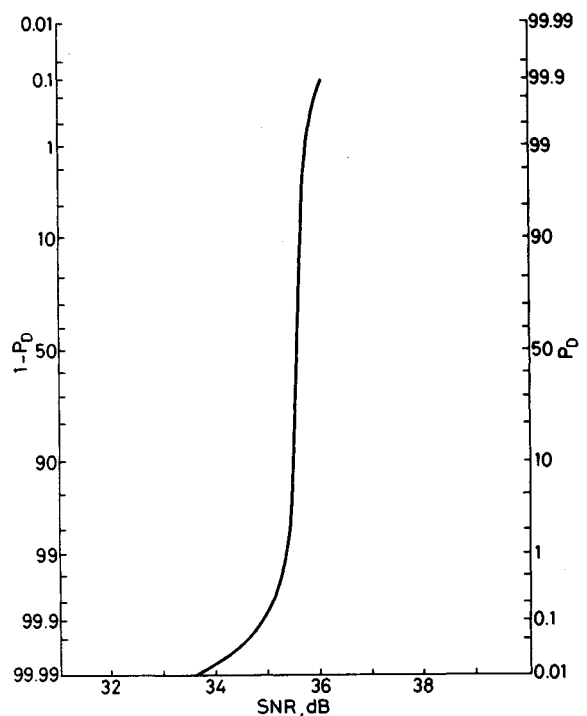

Fig. 13 *Detection performance of a Swerling 0 target model in log-normal and Rayleigh clutter for processing of three pulses*

CNR = 30 dB, $\rho = 0.9$, $N = 3$, $P_{FA} = 5 \times 10^{-3}$
a Rayleigh   *b* Log-normal

Fig. 15 *Detection performance of a Swerling 0 target model in log-normal clutter for processing of four pulses*

'Rayleigh' curve not shown, requiring tens of decibels less; CNR = 30 dB, $\rho = 0.9$, $N = 4$, $P_{FA} = 2.8 \times 10^{-5}$

refer to the same P_{FA} and $N = 2$, 3 and 4 pulses, respectively. As an example, to obtain a P_D of 90% the input SNR required is 51.8 dB for $N = 2$, and it decreases to 41.8 dB and 35.5 dB for $N = 3$ and 4, respectively. This saving is comparable (but not coincident) with the increase in IF achieved, which evaluates as 13 dB, 23 dB and 31 dB, respectively.

The detection loss of the linear receiver in the presence of log-normal clutter is summarised in Table 3, for a

Table 3: Detection performance degradation SNR loss for $P_D = 80\%$

P_{FA}	N 2	3	4
9×10^{-3}	0	—	—
10^{-3}	10	16	—
1.8×10^{-4}	18	17	16
2.8×10^{-5}	33	25	23

SNR loss in decibels.

required P_D of 80%. It turns out that a dramatic performance degradation is observed, when P_{FA} is very small; conversely, when the number of pulses increases, the loss decreases. A moderate decrease in the loss is also found when P_D increases. As an example, for $N = 3$ pulses and $P_{FA} = 2.8 \times 10^{-5}$, when P_D ranges between 0.5 and 0.99 the loss is between 25 and 23 dB, respectively.

The performance of the conventional processor has finally been evaluated for a scan-to-scan fluctuating target (Swerling 1 model) with Rayleigh amplitude. The optimum processor, in the presence of Gaussian noise, is the same as depicted in Fig. 7, with some performance degradation due to target fluctuation. The detection performance in the presence of log-normal clutter is represented in Figs. 16 and 17. In particular, in Fig. 16 a comparison is made between the performance achieved for the target and clutter models. It is evident that, for a log-normal clutter, the shape of the curve for Swerling 1 target (curve b) shows a much slower
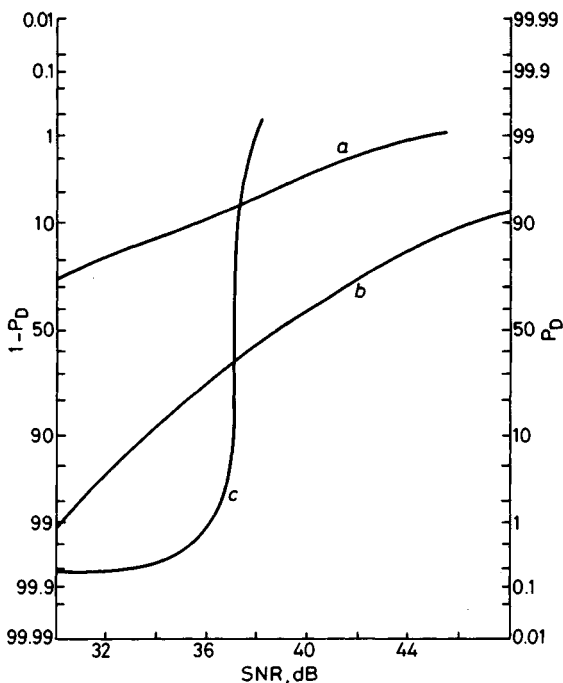

Fig. 16 *Comparison of detection performance for different models of target and clutter*

Case for Swerling 0 target and Rayleigh clutter is not shown, requiring tens of decibels less; CNR = 30 dB, $\rho = 0.9$, $N = 2$, $P_{FA} = 10^{-3}$
a Swerling 1 target and Rayleigh clutter
b Swerling 1 target and log-normal clutter
c Swerling 0 target and log-normal clutter

increase in P_D when the SNR increases, with respect to the fixed target (c). Furthermore, in the range of $P_D = 0.8$–0.9, a fluctuation loss of 6–10 dB results. In the same Figure, the curve (a) of P_D against SNR for a Swerling 1 target in the presence of Rayleigh clutter is shown, for comparison. For $P_D = 0.8$, the loss due to the log-normal distribution amounts to 12 dB (compare curves a and b). Fig. 17 shows
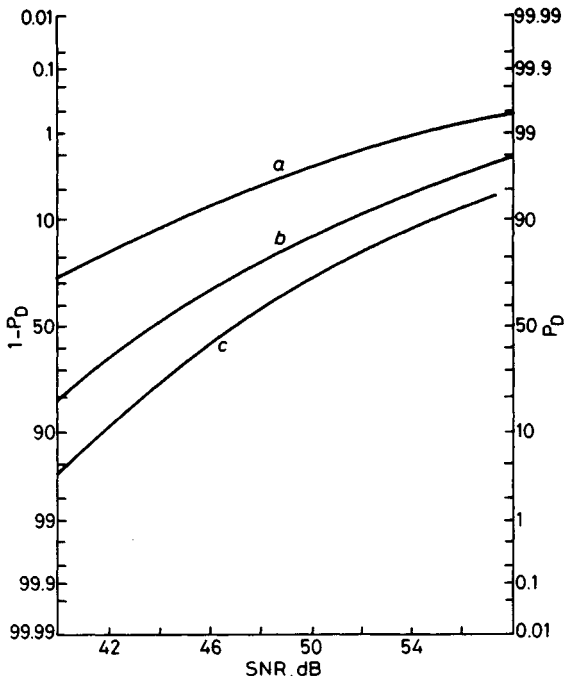

Fig. 17 *Comparison of detection performance of a Swerling 1 target model in log-normal clutter for different values of P_{FA} and N*

CNR = 30 dB, $\rho = 0.9$
a $P_{FA} = 1.8 \times 10^{-4}$ and $N = 3$
b $P_{FA} = 2.8 \times 10^{-5}$ and $N = 3$
c $P_{FA} = 1.8 \times 10^{-4}$ and $N = 2$

some curves of P_D against SNR for fluctuating targets and log-normal clutter, which allow comparison among different values of P_{FA} and number N of pulses. In particular, for $P_D = 90\%$, increasing the number of pulses to three (curves a and c) provides a saving of 10 dB in SNR (again comparable with the increase in IF), while a reduction of P_{FA} of nearly one order of magnitude implies an extra of 6–7 dB in SNR (curves a and b).

Suboptimal linear filters (e.g. binomial MTI or coherent integrator implemented by means of FFT technique) have not been considered in this Section, although they are the most common approximation to the optimum filters (eqn. 33). However, the performance degradation of these filters with respect to the optimum ones is well known [1] and is related to the reduced improvement factor achieved.

4 Nonlinear canceller of log-normal clutter

The detection probability curves evaluated in Section 3 show the limited performance of a conventional processing chain with respect to log-normal clutter. The linear processor, upstream of the envelope detector, is optimum for clutter having Rayleigh amplitude distribution [2] and cannot perform well against disturbances having non-Rayleigh amplitude distribution. This observation motivates the attempt made in this Section of using a nonlinear filter to cancel log-normal clutter.

Derivation of the proposed nonlinear scheme exploits the techniques of homomorphic filtering and linear prediction error filters, well known and widely applied in communications and radar (see Reference 37, Chap. 10).

Moreover, it can be shown that the same structure can be derived as a particular case from a very general approach, based on the estimator-correlator receiver, discussed in Reference 20 and applied to clutter and target models in References 20 and 28. Here, it is preferred to derive the processor by resorting to intuition, the goal being to design a near-optimal prediction scheme for clutter samples, according to a mean-square error criterion.

It is worth pointing out that resorting to nonlinear filters allows processing of the data in such a way that not only second-order statistics (e.g. spectra) are relevant, but higher-order moments are properly accounted for. This, for non-Gaussian signals, allows a more appropriate 'cancellation' of the process or, equivalently, more adequate control of the PDF of the statistic used for the decision.

To illustrate the rationale behind the proposed approach, consider the schematic diagram of Fig. 18.
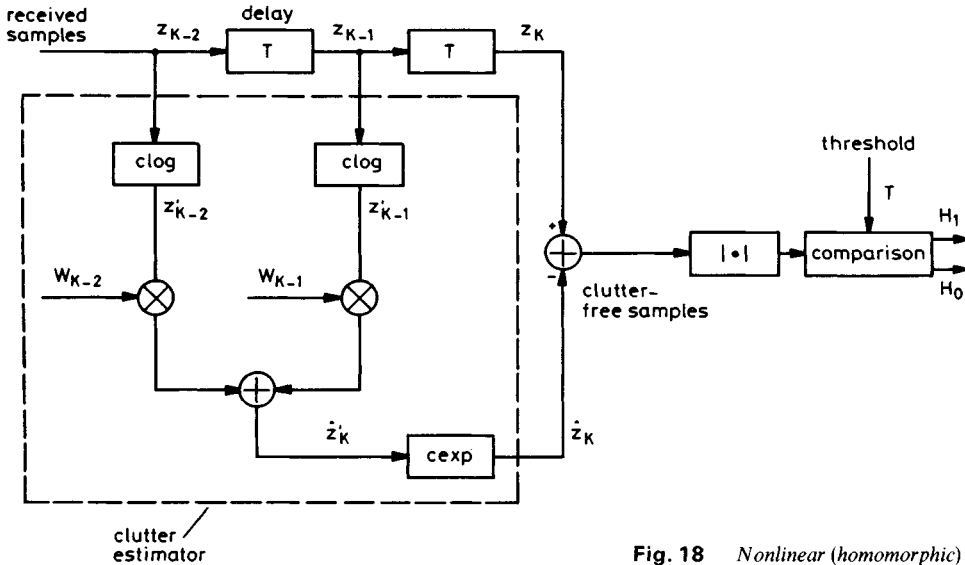
$$\begin{bmatrix} w_{k-2} \\ w_{k-1} \end{bmatrix} = (M'_r)^{-1} R \qquad (35)$$

where the matrix M'_r and the vector R are derived by the same matrix M' (3×3) as follows:

$$M' = \begin{bmatrix} m'_{11} & m'_{12} & m'_{13} \\ m'^{*}_{12} & m'_{22} & m'_{23} \\ \hline m'^{*}_{13} & m'^{*}_{23} & m'_{33} \end{bmatrix} = \begin{bmatrix} M'_r & R \\ \hline R^{T*} & m'_{33} \end{bmatrix} \qquad (36)$$

(c) The output of the linear filter is passed through an instantaneous nonlinear block which performs the complex exponential (cexp) function. The estimate $\hat{z}_k$ of the kth received sample is thus provided. Clutter-free samples are obtained by subtracting from the incoming data sample z_k the estimate $\hat{z}_k$. The output from this new MTI

Fig. 18 Nonlinear (homomorphic) clutter canceller

Three received samples z_k, z_{k-1} and z_{k-2} are processed, the extension to a longer data batch being straightforward. The purpose is to process the samples z_{k-1} and z_{k-2} in order to give an estimate $\hat{z}_k$ of the kth received sample. If the clutter/signal-plus-noise ratio is high enough, the quantity $\hat{z}_k$ corresponds to the estimated clutter sample at the kth step, and the clutter cancellation is achieved by the simple operation $(z_k - \hat{z}_k)$.

The estimate $\hat{z}_k$ is obtained by means of the following three steps:

(a) z_{k-1} and z_{k-2} are passed through two nonlinear instantaneous blocks performing the inverse of the nonlinear function of the model in Fig. 5b, namely the complex logarithm (clog) function. The outputs z'_{k-1} and z'_{k-2} are now Gaussian-distributed, with zero mean and a covariance matrix M'_r (2×2) which can be directly derived by the covariance matrix M' (3×3):

$$M' = E\{(z')^{*}(z')^{T}\} \qquad (34)$$

where $z' = (z'_{k-2} \, z'_{k-1} \, z'_k)^{T}$

The matrix M' is equal to M_z, which was used in Section 2 to generate log-normal clutter (eqn. 23), neglecting the presence of thermal noise and target in z_k, z_{k-1}, z_{k-2}.

(b) The samples z'_{k-1} and z'_{k-2} can be linearly processed in order to predict, one step ahead, the sample z'_k. This is achieved by means of a transversal filter having weights w_{k-1} and w_{k-2}, which are evaluated according to a mean-square error criterion as follows (Reference 40, p. 691, eqn. 1.4):

device can be envelope-detected and compared with a suitable threshold. The proposed approach provides only the clutter cancellation, while signal enhancement is not achievable in the coherent section of the processor. However, a noncoherent integration of target echo could be inserted after the modulus extraction; this case is not considered in the remaining part of the paper.

It is worth considering the matching between the model (with well separated memory and nonlinearity) and the cancellation filter (characterized again by a separation between nonlinearity and memory). Furthermore, it is necessary to spend a few words on the Gaussian variates z' purposely obtained in the receiver. They reproduce the corresponding Gaussian-distributed and correlated samples of the model (if noise and target echo can be neglected).

The relationship between the covariance matrices M (referred to as M_w in Section 2.3), pertaining to the environment, and M' (denoted by M_z in Section 2.3), pertaining to the model and to the reproduced values z', is known (eqn. 23) and used to design the prediction filter. However, when comparing the performance of a same processor (e.g. MTI) against Rayleigh and log-normal clutter, the same matrix M must be considered for both clutter models, in order to have a fair comparison pertaining to the same spectrum. This was not done in Reference 22, where the Rayleigh clutter was assumed to have covariance matrix M' (more correlated than M), giving rise to an unfair comparison.

79

The detection performance of the processor of Fig. 18 has been evaluated by means of computer simulation. The following three situations have been considered and compared:

(a) Log-normal clutter processed by the nonlinear filter of Fig. 18.

(b) Log-normal clutter processed by a conventional linear (binomial) MTI.

(c) Rayleigh amplitude clutter processed by a conventional linear MTI (this case is taken as a term of reference).

The same one-lag correlation coefficient (in the example considered, $\rho = 0.9$) and the same clutter/noise ratio (CNR = 30 dB) have been assumed for the above-mentioned situations. Additionally, it has been considered that the amplitude of the target echo is constant and the Doppler frequency is randomly distributed in $[0, 1/T]$ and variable from pulse to pulse.

The threshold values plotted against the probability of false alarm are shown in Fig. 19 for the three situations considered. It can be noted that the situation (c) is the
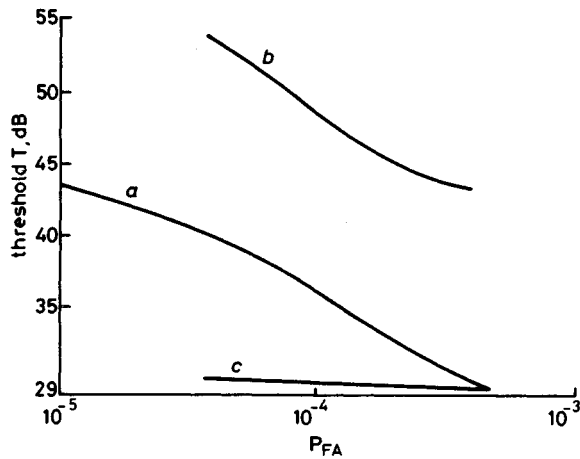
most favoured; situations (a) and (b) require a higher threshold in order to maintain the same value of PFA. However, the case (a) performs better than case (b), as is confirmed in Fig. 20. Here the detection probability is plotted against the signal/noise ratio value when the PFA value is 3.6×10^{-4}. It can be seen that the nonlinear filter allows a saving of about 10 dB in SNR with respect to the linear conventional MTI when log-normal clutter is processed. A smaller gain (about 5 dB on average) can be achieved in the case of P_{FA} equal to 3.8×10^{-5}, as shown in Fig. 21. Another set of detection performance curves (Fig. 22) has been derived for a target signal represented as

Fig. 19   *Threshold values against P_{FA} values*

CNR = 30 dB, $\rho = 0.9$, $N = 3$
a Log-normal clutter, processor of Fig. 18
b Log-normal clutter, processor of Fig. 7
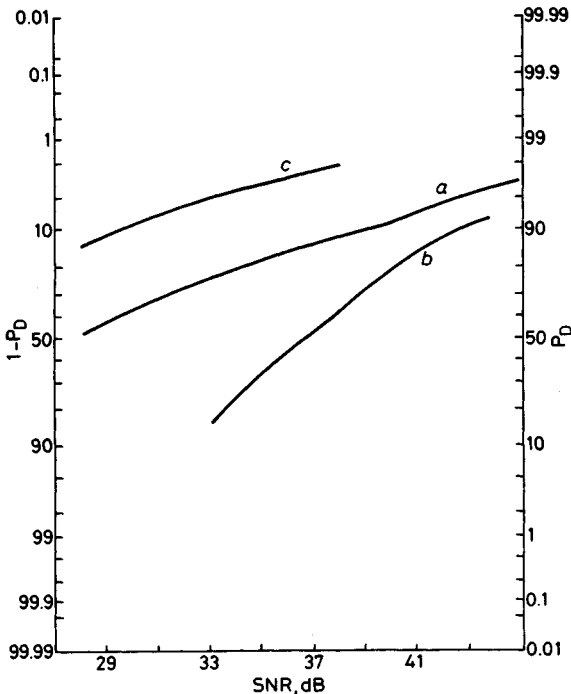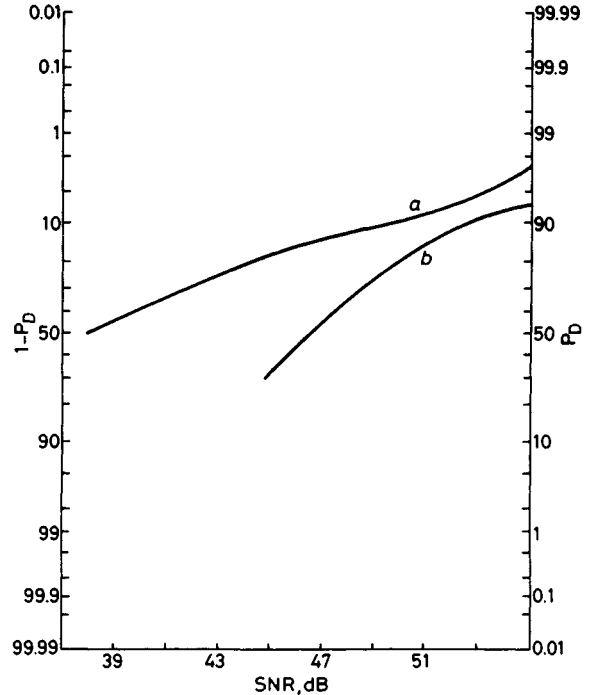c Rayleigh clutter, processor of Fig. 7

Fig. 21   *Detection performance at $P_{FA} = 3.8 \times 10^{-5}$*

Meaning of curves (a) and (b) same as in Fig. 19 (performance of processor (c) is off the scale); CNR = 30 dB, $\rho = 0.9$, $N = 3$
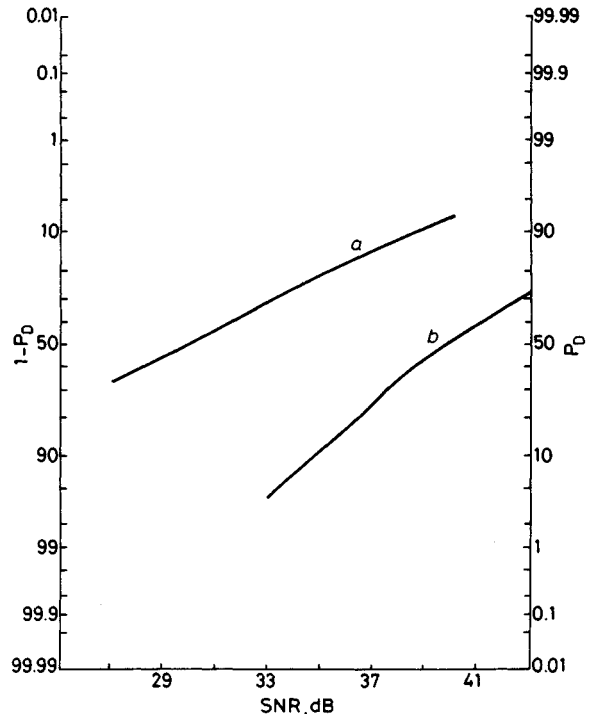
Fig. 20   *Detection performance at $P_{FA} = 3.6 \times 10^{-4}$*

Meaning of curves (a)–(c) same as in Fig. 19; CNR = 30 dB, $\rho = 0.9$, $N = 3$

Fig. 22   *Detection performance for Swerling 2 target model*

Meaning of curves (a) and (b) same as in Fig. 19 (performance of processor (c) is off the scale); CNR = 30 dB, $\rho = 0.9$, $P_{FA} = 1.4 \times 10^{-4}$, $N = 3$

a Swerling 2 model. The clutter source is the same as in the previous example. The detection threshold has been selected to obtain a P_{FA} value of 1.4×10^{-4}. This limited number of examples demonstrates that nonlinear filtering provides a useful approach to improve detection performance of radar systems in log-normal clutter.

A final remark to be considered refers to the fact that the covariance matrix M' of the samples z'_k, z'_{k-1}, z'_{k-2} is a priori unknown. A usual approach to this problem leads to the adaptive processor, which estimates the covariance matrix on-line and efficiently evaluates the filter weights W. An exhaustive overview of the possible adaptive techniques to be employed can be found in Reference 27. Here it is sufficient to consider the schematic diagram of the adaptive processor, which is shown in Fig. 23. The adap-
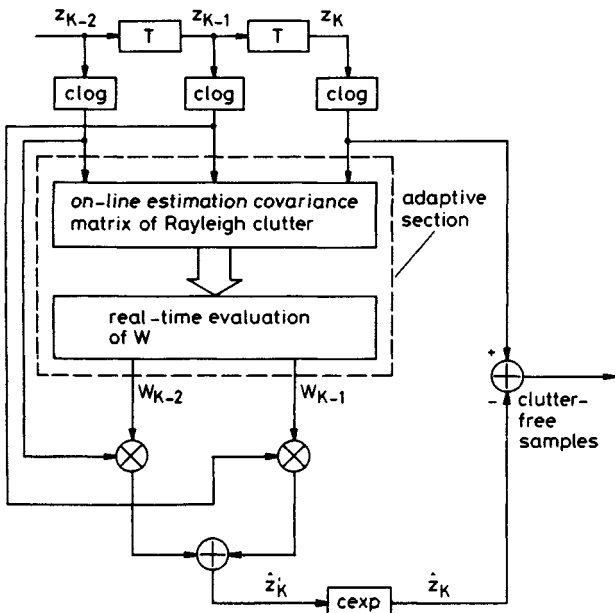

Fig. 23 *Adaptive approach to log-normal clutter cancellation*

tive section, indicated in the Figure, represents the novel part with respect to the previous schematic diagram of Fig. 18. Preliminary results concerning the robustness and adaptive implementation of the proposed nonlinear processor are available in Reference 46.

5   Conclusions and trends of research

In this paper the problem of target detection in log-normal clutter has been considered in detail. A breakthrough in the theory has been achieved by introducing a coherent model for the log-normal clutter. The model, i.e. the cascade of a linear dynamic filter and a nonlinear instantaneous filter fed by a white Gaussian process, is quite general. It can be extended to other non-Rayleigh clutter, such as Weibull clutter, by a suitable modification of the nonlinearity shape and of the parameters of the linear filter. Another relevant result has been the evaluation of performance of conventional processors fed by log-normal clutter in a number of operational cases of interest. A nonlinear MTI canceller (and a schematic diagram of it) providing better performance with respect to the linear one has also been suggested.

The theory developed in this paper needs some more investigation in the areas of:

(a) clutter modelling.

(b) performance evaluation.

(c) optimum detection scheme.

The first item (a) is strictly connected to the clutter sample generation by means of a digital computer. Two problems arise in this respect, namely (i) mathematical refinements of clutter modelling to avoid mathematical expedients discussed in Section 2.3, and (ii) extension of the computer generation method to other relevant clutter models such as Weibull and K-distribution.

With reference to the performance evaluation task (b), the complexity of the problem in hand makes any mathematical evaluation impracticable. At the same time, Monte Carlo simulation requires a large number of independent statistical trials, whose number increases very much as the P_{FA} value decreases. It should be considered the opportunity of alternative methods such as the importance sampling technique [38].

The latter simulation technique needs some comments in order to have the feeling of the problems which arise in using it. Briefly speaking, importance sampling is an efficient method to estimate low P_{FA} values. This objective is achieved by artificial generation of 'important' events (i.e. false alarms) through a deliberate distortion, called biasing, of the statistics of the underlying processes. Of course, at the very end, the false alarm count must be properly unbiased [38]. A synthesis of biasing and unbiasing procedures is the crucial point of the method. The fulfilment of this task requires having a formal expression, at least, of the probability of false alarm, and to recognise in this formal expression the weights for biasing the original process to compare with the threshold. As far as the processors of Figs. 7 and 18 are concerned, these two problems are really hard to solve. Furthermore, evaluation of the confidence of importance sampling simulation results is another major concern.

The final point to be considered is the derivation of optimum detection schemes to deal with any type of clutter and target models [45]. A first attempt in this direction is due to Schleher and Kozin [39], who apply the theory of stochastic filtering to this complex detection problem. Their approach, however, is limited to the real-valued continuous-time signal case. Another limitation refers to the assumption of completely known target signal when competing with clutter.

A powerful generalisation of this approach is available in Reference 28, which represents the first systematic approach, as far as the authors are aware, to the processing of clutter and target signals having any type of probability density and autocorrelation functions. Briefly, the rationale behind the proposed approach is to replace the original complex test of hypotheses, built around the received radar echoes, with a test of hypotheses operating on two white Gaussian noise processes having different variances and mean values. The two white Gaussian processes correspond to the residuals (statistical innovation) obtained by estimating the expected received radar echoes in the two alternative hypotheses. It is shown [28] that, in the log-normal clutter case, the architectures of the two estimators are very similar to the homomorphic filter depicted in Fig. 18.

6   Acknowledgment

7 References

1 SCHLEHER, D.C.: 'MTI radar' (Artech House, Dedham, MA, USA, 1978)
2 BRENNAN, L.E., and REED, I.S.: 'Theory of adaptive radar', *IEEE Trans.*, 1973, **AES-9**, pp. 237–252
3 FARINA, A., and STUDER, F.A.: 'Application of Gram-Schmidt algorithm to optimum radar signal processing', *IEE Proc. F, Commun., Radar & Signal Process.*, 1984, **131**, (2), pp. 139–145
4 LONG, M.W.: 'Polarization and statistical properties of clutter'. Proceedings of international symposium on noise and clutter rejection in radar and imaging sensors, Tokyo, October 1984, pp. 25–32
5 LONG, M.W.: 'Radar reflectivity of land and sea' (Artech House, 1975)
6 JAKEMAN, E., and PUSEY, P.N.: 'A model for non-Rayleigh sea echo', *IEEE Trans.*, 1976, **AP-24**, pp. 806–814
7 JAO, J.K.: 'Amplitude distribution of composite terrain radar clutter and the K-distribution', *ibid.*, 1984, **AP-32**, pp. 1049–1062
8 SCHLEHER, D.C.: 'Automatic detection and radar data processing' (Artech House, 1980)
9 SEKINE, M., MUSHA, T., TOMITA, Y., HAGISAWA, T., IRABU, T., and KIUCHI, E.: 'On Weibull distributed weather clutter', *IEEE Trans.*, 1979, **AES-15**, pp. 824–828
10 PERRY, J.L.: 'Modern radar clutter suppression techniques: a comparison of theoretical and measured results'. Proceedings of international conference on radar, Paris, 1984, pp. 485–497
11 TRUNK, G.V.: 'Detection of targets in non-Rayleigh sea clutter'. Proceedings of EASCON, 1971, pp. 239–245
12 TRUNK, G.V.: 'Radar properties of non-Rayleigh sea clutter', *IEEE Trans.*, 1972, **AES-8**, pp. 196–204
13 TRUNK, G.V., and GEORGE, S.F.: 'Detection of targets in non-Gaussian sea clutter', *ibid.*, 1970, **AES-6**, pp. 620–628
14 TRUNK, G.V.: 'Modification of "radar properties of non-Rayleigh sea clutter"', *ibid.*, 1973, **AES-9**, p. 110
15 FAY, F., CLARKE, J., and PETERS, R.: 'Weibull distribution applied to sea clutter'. *IEE Conf. Publ. 155* (Radar '77), London, 1977, pp. 101–104
16 WARD, K.D.: 'A radar sea clutter model and its application to performance assessment'. *IEE Conf. Publ. 216* (Radar '82), London, October 1982, pp. 203–207
17 CHAN, H.C.: 'Multi-frequency measurement of radar sea clutter at shallow grazing angles'. AGARD conference preprint 364 on 'Target signature', London, October 1984, pp. 2-1, 2-14
18 WARD, K.D., and WATTS, S.: 'Radar clutter in airborne maritime reconnaissance systems'. Proceedings of conference on military microwaves, October 1984, pp. 222–228
19 EWELL, G.W., TULEY, M.T., and HORNE, W.F.: 'Temporal and spatial behaviour of high resolution sea clutter spikes'. Proceedings of IEEE national radar conference, Atlanta, GA, March 1984, pp. 100–104
20 SCHLEHER, D.C.: 'Radar detection in log normal clutter'. Ph.D dissertation, Polytechnic Institute of New York, June 1975
21 SCHLEHER, D.C.: 'Radar detection in log normal clutter'. Proceedings of IEEE international radar conference, Washington, DC, 1975, pp. 262–267
22 SCHLEHER, D.C.: 'MTI detection performance in Rayleigh and log normal clutter'. Proceedings of IEEE international radar conference, Washington, DC, 1980, pp. 299–304
23 SCHLEHER, D.C.: 'Harbor surveillance radar detection performance', *IEEE J. Oceanic Eng.*, 1977, **OE-2**, pp. 318–325
24 SCHLEHER, D.C.: 'MTI detection loss in clutter', *Electron. Lett.*, 1981, **17**, pp. 82–83
25 FANTE, R.L.: 'Probability of detecting a fluctuating target immersed in both noise and clutter', *IEEE Trans.*, 1977, **AES-13**, pp. 711–716
26 SCHLEHER, D.C.: 'Radar detection in Weibull clutter', *ibid.*, 1976, **AES-12**, pp. 736–743
27 FARINA, A., and STUDER, F.A.: 'Adaptive implementation of optimum radar signal processor'. Proceedings of international conference on radar, Paris, 1984, pp. 93–102
28 FARINA, A., RUSSO, A., and STUDER, F.A.: 'Advanced models of targets and disturbances and related radar signal processors'. Proceedings of IEEE international radar conference, Washington, DC, May 1985, pp. 151–158
29 POLLON, G.E.: 'Statistical parameters for scattering from randomly oriented arrays, cylinders, and plates', *IEEE Trans.*, 1970, **AP-18**, pp. 68–75
30 HARGER, O.R.: 'On the characterization and likelihood functional of log normal random processes', *ibid.*, 1970, **IT-16**, pp. 630–632
31 PAPOULIS, A.: 'Probability, random variables, and stochastic processes' (McGraw-Hill, New York, 1965)
32 RUSSO, A.: 'Analisi e valutazione delle prestazioni di ricevitori per echi radar in presenza di disturbi Gaussiani e lognormali'. E.E. degree thesis, University of Naples, 1983 (in Italian)
33 SZAJNOWSKI, W.J.: 'Generation of correlated log-normal clutter samples', *Electron. Lett.*, 1976, **12**, pp. 497–498
34 PEEBLES, P.: 'The generation of correlated log normal clutter for radar simulation', *IEEE Trans.*, 1971, **AES-7**, pp. 1215–1217
35 LIU, B., and MUNSON, D.C.: 'Generation of a random sequence having a jointly specified marginal distribution and autovariance', *ibid.*, 1982, **ASSP-30**, pp. 973–983
36 CASAR CORREDERA, J.R., ALCAZAR, J.M., and FIGUERAS-VIDAL, A.R.: 'Some simple nonlinear prediction schemes', in 'Digital signal processing — 84' (Elsevier Science Publishers BV), pp. 348–352
37 OPPENHEIM, A.V., and SCHAFER, R.W.: 'Digital signal processing' (Prentice-Hall, Englewood Cliffs, NY, USA, 1975)
38 JERUCHIM, M.C.: 'Techniques for estimating the bit error rate in the simulation of digital communication systems', *IEEE J. Sel. Areas Commun.*, 1984, **SAC-2**, pp. 153–169
39 SCHLEHER, D.C., and KOZIN, F.: 'Radar signal processing using digital nonlinear filters'. Proceedings of IEEE international conference on acoustic speech and signal processing, Hartford, USA, May 1977, pp. 854–858
40 FARINA, A.: 'Single sidelobe canceller: theory and evaluation', *IEEE Trans.*, 1977, **AES-13**, pp. 690–699
41 SZAJNOWSKI, W.J.: 'Discrimination between log normal and Weibull clutter', *ibid.*, 1977, **AES-13**, pp. 480–485
42 AL-HUSSAINI, E., BADRAN, F., and TURNER, L.: 'The nonparametric detection of signals embedded in log-normal noise', *ibid.*, 1978, **AES-14**, pp. 668–670
43 EKSTROM, J.: 'The detection of steady state targets in Weibull clutter', *IEE Conf. Publ. 105* (Radar present and future), London, 1973, pp. 221–226
44 CHEN, P., and MORCHIN, W.: 'Detection of targets in noise Weibull clutter background'. NAECON conference record, May 1977, pp. 929–933
45 FANTE, R.L.: 'Detection of multiscatter targets in k-distributed clutter', *IEEE Trans.*, 1984, **AP-32**, pp. 1358–1363
46 MORABITO, F.C.: 'Analisi e sintesi di algoritmi non lineari e adattivi per la detezione di segnali radar in ambienti non Gaussiani'. E.E. degree thesis, University of Naples, 1985 (in Italian)

8 Appendix

8.1 Evaluation of joint PDF of (u, v)

Consider the transformation of variables

$$u = e^x \cos y = f(x, y)$$

$$v = e^x \sin y = g(x, y) \tag{37}$$

where x, y are independent zero-mean Gaussian variates.

According to Reference 31 (Section 7-2, p. 201), the PDF $p(u, v)$ can be evaluated, provided that a countable number of solutions (x_i, y_i) exist for (x, y) for any pair (u, v) as follows:

$$p(u, v) = \sum_i \frac{p_{xy}(x_i, y_i)}{|J(x_i, y_i)|} \tag{38}$$

where $J(x_i, y_i)$ denotes the Jacobian of the transformation, evaluated in the ith solution.

In the present case, inverting $f(x, y)$ and $g(x, y)$ yields

$$\left. \begin{aligned} x_i &= \tfrac{1}{2} \ln (u^2 + v^2) \\[1em] y_i &= \tan^{-1} (v/u) + \frac{\pi}{2} (1 - \mathrm{sign}\, (u)\, \mathrm{sign}\, (v) + i 2\pi \end{aligned} \right\} \tag{39}$$

since, from the couple (u, v), the value of y is determined in the interval $[-\pi, \pi]$.

The Jacobian of the transformation evaluates as

$$|J(x_i, y_i)| = \exp (2x_i) = (u^2 + v^2) = |w|^2 \tag{40}$$

independently of i. Hence, each term in the summation contributes to $p(u, v)$ as follows:

$$\frac{p(x_i, y_i)}{|J(x_i, y_i)|} = \frac{1}{2\pi\sigma^2} \frac{1}{(u^2 + v^2)} \exp \left\{ -\frac{x_i^2}{2\sigma^2} \right\}$$

$$\times \exp \left\{ -\frac{y_i^2}{2\sigma^2} \right\} \tag{41}$$

Taking into account the explicit expressions (eqn. 39) of x_i and y_i, from eqn. 38 the expression (eqn. 12) of $p(u, v)$ follows.

8.2 Evaluation of statistics of w

Assume that (x, y) are zero-mean, jointly distributed Gaussian variates, with standard deviations σ_x, σ_y and a correlation coefficient ρ between them. Evaluation of $E\{w\}$ requires the computation of

$$E\{w\} = \frac{1}{2\pi\sigma_x\sigma_y\sqrt{(1-\rho^2)}} \iint\limits_{-\infty}^{+\infty} e^{(x+jy)}$$

$$\times\ e^{[(x^2/\sigma_x^2)+(y^2/\sigma_y^2)-2\rho(xy/\sigma_x\sigma_y)]/2(1-\rho^2)}\ dx\ dy \qquad (42)$$

which can be solved by using the relationship

$$\int_{-\infty}^{+\infty} e^{-p^2y^2}e^{\pm qy}\ dy = \frac{\sqrt{\pi}}{p}\ e^{q^2/4p^2} \qquad (43)$$

with the following assumptions:

$$p^2 = \frac{1}{2\sigma_y^2} \quad q = j + \frac{\sigma_x}{\sigma_y}\rho \qquad (44)$$

Then it follows that

$$E\{w\} = c\exp\{\tfrac{1}{2}(\sigma_x^2 - \sigma_y^2) + j\sigma_x\sigma_y\rho\} \qquad (45)$$

which coincides with eqn. 10, where σ_{xy} represents $\sigma_x\sigma_y\rho$.

In order to evaluate $E\{|w|^2\}$, recall that, according to the definition of eqn. 8, it turns out that

$$|w|^2 = e^{2x} \qquad (46)$$

and, since the marginal distribution of x is Gaussian, with zero mean and variance σ_x^2, the required expectation is

$$E\{|w|^2\} = \frac{1}{\sqrt{(2\pi)}\sigma_x} \int_{-\infty}^{+\infty} \exp\left(2x - \frac{x^2}{2\sigma^2}\right) dx \qquad (47)$$

This is easily solved, resorting again to eqn. 43 with the new positions

$$p^2 = \frac{1}{2\sigma_x^2} \quad q = 2 \qquad (48)$$

giving rise to eqn. 11.